

Application of a multi-variable optimization method to determine lift-up design for optimum wind comfort

Yaxing Du^a, Cheuk Ming Mak^{a*}, Yantong Li^b

^aDepartment of Building Services Engineering, The Hong Kong Polytechnic University, Hung Hom, Kowloon, Hong Kong

^bDepartment of Architecture and Civil Engineering, City University of Hong Kong, Tat Chee Avenue, Kowloon, Hong Kong

*Corresponding author email: cheuk-ming.mak@polyu.edu.hk

Abstract

The lift-up building design has been demonstrated to provide favorable wind comfort, but there is a lack of investigation on optimum wind comfort condition. This study coupled computational fluid dynamics (CFD) technique and response surface methodology (RSM) to determine the most desirable wind comfort around an isolated building with lift-up design. A multi-variable optimization method is proposed to determine optimum wind comfort and the corresponding lift-up design variables, namely, lift-up height (H_L), core aspect ratio (AR) and core number (N). To better illustrate wind comfort around the building, the wind comfort in the lift-up area and the podium area are investigated separately. The Detached Eddy Simulation (DES) approach is employed throughout the whole CFD simulation process. The quality and goodness of the established RSM models are examined by analysis of variance and genetic algorithm is applied to generate optimal design solution. The generated results illustrate good performance of the established RSM model. Results show that the optimum wind comfort is obtained when H_L is 8m, AR is 10%, and N is 6. The lift-up core aspect ratio is subsequently found to have greatest effect on wind comfort among the three design variables in both the lift-up area and the podium area. In addition, the proposed method is applicable to other similar environmental design conditions and the outcomes of study can also be of great value in the improvement of wind comfort in compact urban cities.

Keywords: *Lift-up design; wind comfort; computational fluid dynamics (CFD); response surface methodology (RSM); multi-variable optimization method.*

Nomenclature

A	Area of the target region, (m^2)	$U_{i,j}$	Velocity gradients, (s^{-1})
AR	Lift-up core aspect ratio, (-)	U_p	Mean wind velocity at pedestrian level, (m/s)
C_{D1}, C_{D2}	Constants of S-A eddy viscosity model, (-)	U_r	Mean wind velocity at reference height, (m/s)
c_w	Empirical constant, (-)	W_B	Building width, (m)
C_{DES}	Model constant, (-)	W_c	Lift-up core width, (m)
d	Distance from first node to wall surface, (m)	x	Design variable of RSM model, (-)
\tilde{d}	New length scale parameter of DES model, (m)	Z	Vertical height, (m)
f_w	Wall destruction function, (-)	ε	Statistical error of RSM model, (-)
f_{v1}	Intermediate variable, (-)	$\tilde{\beta}$	Estimated parameter of RSM model, (-)
H_B	Building height, (m)	η	Estimated value of RSM model, (-)
H_L	Lift-up height, (m)	ρ	Air density, (Kg/m^3)
I	Turbulence intensity, (-)	ν	Turbulent viscosity, (Pa s)
L_B	Building length, (m)	$\tilde{\nu}$	New turbulent viscosity variable, (Pa s)
L_c	Lift-up core length, (m)	κ	Von Karman's constant, 0.4187
MVR	Mean wind velocity ratio, (-)	μ_t	Eddy viscosity, (Pa s)
\overline{MVR}	Area-weighted MVR value, (-)	ν_t	Kinematic eddy viscosity, (m^2/s)
MVR'	MVR value at specific location, (-)	τ_{ij}	Sub-grid scale stress term, (-)
\overline{MVR}_L	Area-weighted MVR value in lift-up area, (-)	Δt	Time step, (s)
\overline{MVR}_P	Area-weighted MVR value in podium area, (-)	t^*	Non-dimensional sampling time unit, (-)
N	Lift-up core number, (-)	χ	Intermediate variable, (-)
P	Pressure, (Pa)		
t	Time, (s)		
u_i, u_j	Velocity component, (m/s)		
U	Mean wind velocity, (m/s)		

Introduction

With the rapid progress of urban development, modern mega-cities are teeming with tall and closely spaced buildings, which subsequently results in congested air flow at the pedestrian level. The limited air circulation at pedestrian level has caused serious problems, including wind and thermal discomfort [1-3], and accumulated air pollutants [4-6]. The deterioration of pedestrian level wind environment is very serious in Hong Kong, where tall buildings and bulky developments are closely spaced. Thus, the Air Ventilation Assessment (AVA) scheme [7] was stipulated in Hong Kong to enhance the pedestrian level wind velocity and new wind comfort criteria [8] have been proposed for the purpose of improving wind comfort. In contrast to the uncomfortable wind environment caused by windy conditions, which has long been academically researched [9-11], the unacceptable environment resulting from widespread stagnant wind flow has received increasing awareness and concerns [6, 8, 12-14]. Therefore, improving the pedestrian level wind comfort in high-rise compact urban areas, like Hong Kong, has become a pressing issue for city planners and architects.

To improve wind comfort at pedestrian level, the lift-up building design has been used as a promising solution that does not sacrifice the available space inside a building. The lift-up design, which forms an open space between the ground and the main building structures, has been widely adopted in building designs in southern China and south-eastern Asia. This can be accounted for its remarkable feature of providing favorable microclimate for wind and thermal comfort due to its wind amplification and shading effects, as demonstrated in our previous studies [1, 2, 15-18]. Niu et al. [1] documented that the lift-up design can provide local cooling spots in hot and humid summer, which can then be used for some outdoor activities, as indicated in Fig.1. Liu et al. [15, 16] investigated the pedestrian level wind flow around an isolated building using different turbulence models in CFD simulation, including steady-state Reynolds Averaged Navier-Stokes (RANS), unsteady-state RANS (URANS) and detached eddy simulation (DES). It has been found that the pattern and unsteady fluctuation of the wind flow around the building with lift-up design could be reasonably reproduced with DES modelling technique. Du et al. [2] utilized an integrated method to assess the effects of lift-up design on pedestrian level wind environment in a complex university campus. The obtained findings demonstrated that the lift-up design in the campus could improve the low wind environment at pedestrian level in both lift-up area and podium area. In addition, Du et al. [3] performed numerical simulations to quantitatively study the effects of lift-up design in various building configurations on the pedestrian level wind comfort. Tse et al. [18] conducted wind

tunnel tests to study the effects of different lift-up dimensions on pedestrian level wind environment. However, the above investigations mainly utilized qualitative analysis methods and only one factor changed at a time. Moreover, no quantitative relationship was established between two or more lift-up design variables and wind comfort. Thus, in order to obtain the optimum wind comfort by changing the geometric configurations of lift-up design, a quantitative model between the lift-up design variables and wind comfort should be established.

As a well-recognized technique to build approximations of independent design variables and respondent results, the response surface methodology (RSM) has been widely used in the field of computer experiments [19]. Its advantage performance include identification of the mathematical model of multiscale phenomena in various disciplines [20]. The integration of RSM with CFD simulation has launched a new generation of research investigations. Ng et al. [21] evaluated the Air Diffusion Performance Index of a displacement-ventilated office based upon mathematical models developed by RSM and CFD prediction results. In that study, the most influential design parameter was found, and the optimal Air Diffusion Performance Index value was obtained based on the mathematical model. Norton et al. [22] employed RSM and CFD technique to develop a mathematical model to describe the relationship between geometric configuration of a livestock barn and indoor environmental homogeneity. Their results showed that with developed mathematical model, the homogeneity of the indoor environment in a naturally ventilated building is greatly improved. Shen et al. [23, 24] combined CFD simulations with RSM to investigate the ventilation rate of a naturally ventilated livestock. It was found that the approximated mathematical model established by RSM could be used to reasonably represent the ventilation rate of the livestock and could be applied to a system with more variables. Sofotasiou et al. [25] coupled the CFD technique and the RSM optimization technique to determine an optimum window opening design to obtain the optimum ventilation efficiency in a naturally-ventilated building. In that study, the degrees of influence of various design variables were determined and the optimum environmental condition was achieved. Thus, the coupled methodology that combines CFD simulation technique and RSM technique can be utilized to determine the geometric configurations of lift-up design with multiple variables for the optimum wind comfort at pedestrian level.

To assess wind comfort properly, the pedestrian level wind flow around buildings should be accurately predicted. In recent studies, CFD simulation technique has been widely used as an effective alternative approach to reproduce the wind flow around buildings [26-30]. The steady RANS turbulence models have frequently been used for its economic computational costs and

relatively reasonable prediction results [3, 6, 9, 31, 32]. However, some studies have shown that RANS turbulence models may overestimate the wake regions around buildings [27]. Large Eddy Simulation (LES) is generally believed to have better performance than steady RANS turbulence models, but its computing cost is quite expensive for outdoor wind flow prediction [33]. A hybrid RANS/LES turbulence model, namely Detached Eddy Simulation (DES), was then proposed to alleviate the computational cost while preserving the prediction accuracy [34]. Lateb et al. [35] used DES to simulate the flow field and dispersion field from a roof stack, and the results obtained by DES were better overall than those obtained by steady RANS. By comparing the prediction results of wind flow around an isolated building obtained by steady RANS, DES and LES, Liu and Niu [33] clearly indicated that the prediction results of DES has the similar prediction results as LES but with lower computational cost. Kakosimos and Assael [36] conducted several DES validation cases against well-established experimental data, and found that DES approach could simulate the dispersion of gases in a complex terrain. Wu and Niu [37] utilized the DES model to simulate airflow and pollutant dispersion in a group of buildings, and found that the DES model can accurately reproduce the unsteady fluctuation of the air flow around buildings. Therefore, the DES modelling approach is selected in this study to reproduce the wind flow around the building with lift-up design.

In this study, CFD simulation and RSM technique are coupled to determine the geometric configurations of the lift-up design to obtain optimum wind comfort in low wind environment of Hong Kong. A multi-variable optimization method is proposed to achieve optimum wind comfort and to investigate the relationship between the design variables and the respondent results in the meantime. Moreover, the sampling process of the multi-variable optimization method is based on Design of Experiment (DOE) analysis and the Box-Behnken Design (BBD). In addition, the quality and goodness of the fitted RSM model are examined by analysis of variance (ANOVA). Furthermore, the genetic algorithm (GA) is employed to obtain the optimal design solution based on the mathematical model established by RSM. Three design variables of lift-up design are considered during the optimization process: lift-up height (H_L), lift-up core aspect ratio (AR) and number of lift-up core (N). The normalized mean wind velocity parameter (mean velocity ratio, MVR) is chosen for quantitative evaluation of the wind comfort around the building.

The remainder of this paper is organized as follows: after introduction, the methodology of the optimization method is presented in Section 2, and the design variables and objective parameters are introduced in Section 3. Section 4 establishes the accuracy of CFD prediction

results in this study. Section 5 describes the interpretation of the optimization process and discusses of the results, and Section 6 concludes the paper.



Fig.1. Photo of the open space created by lift-up design on a university campus.

2. Methodology

2.1 Response surface methodology (RSM)

As a statistical and mathematical technique, response surface methodology (RSM) has prominent advantages in developing, improving and optimizing procedures, especially with multiple design variables [38]. In general, the complex function relationship between the design variables ($x_1, x_2, x_3, \dots, x_n$) and the corresponding response value (η) can be expressed as the following equation:

$$\eta = g(x_1, x_2, \dots, x_n) + \varepsilon \quad (1)$$

here, ε can be treated as statistical error. By employing the d-order Taylor series approximation model, which also can be seen here as a d-order RSM model, Eq. (1) can be constructed as:

$$\eta = \tilde{\beta}_0 + \sum_{i=1}^n \tilde{\beta}_i x_i + \sum_{i=1}^n \tilde{\beta}_{ii} x_i^2 + \sum_{i=1}^n \sum_{j>i} \tilde{\beta}_{ij} x_j x_i + \sum_{i=1}^n \sum_{j>i} \sum_{k>j} \tilde{\beta}_{ijk} x_k x_j x_i + \dots + \sum_{i=1}^n \tilde{\beta}_{i,\dots,i} x_i^d \quad (2)$$

where, η is the estimated value, and $\tilde{\beta}$ is the estimated parameter for the regression equations. It should be mentioned that the statistical error ε , which originates from incorrect assumption and measurement errors, can be neglected in the computer experiment cases [19]. Thus in this study, Eq. (2) is used to fit the response model instead of Eq. (1).

2.2 Optimization method

The optimization method proposed in this study is a computer simulation-based optimization technique that allows investigation of the optimum design setting with multiple

design variables and manifests the correlations between parameters. The workflow of the multi-variable optimization method is presented in Fig.2, and it has practical extension to similar design problems.

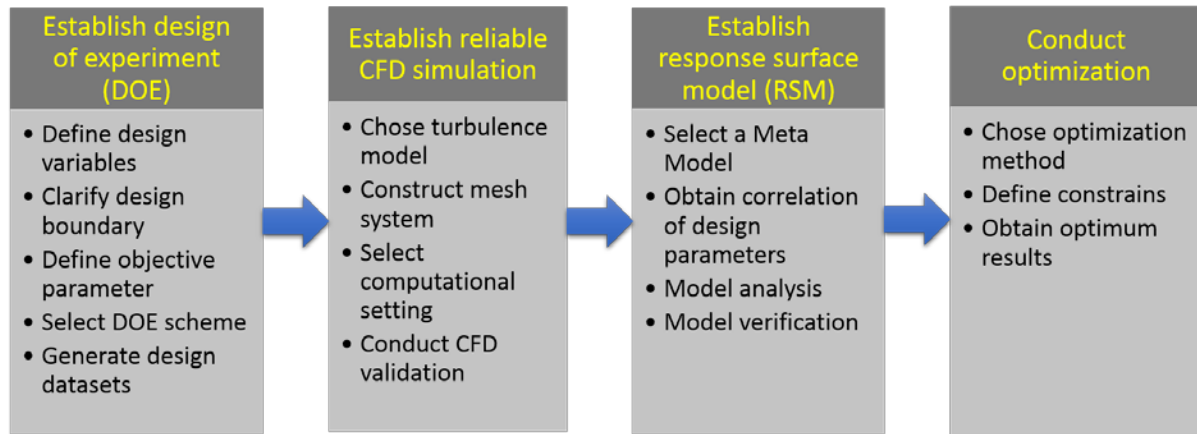


Fig.2. Workflow of the optimization method.

The first step of the optimization method is the establishment of DOE, which can be accomplished by the following steps. (i) The design variables (continuous or discrete) should be defined for the specific problem. In previous studies of lift-up design [2,3,15,18], the lift-up height, the core aspect ratio and the number of cores have been found to play detrimental roles in determining the pedestrian level wind environment, which then influences the wind comfort in the building neighborhood. Thus, the design variables in this study are the lift-up height, the core aspect ratio, and the number of cores. The values for the lift-up height and the core aspect ratio are continues whereas the number of cores is a discrete value. (ii) The boundaries of the design variables should be defined based on the rational criteria. The ranges of the design variables are from 4 to 8 m for the lift-up height, 10% to 70% for the core aspect ratio, and 1 to 6 for the number of cores. The lower bound of the lift-up height is chosen based on the actual lift-up height in a university campus (4 m in prototype) [2,3], and the upper bound is selected based on the height of two stories because the land use efficiency is very important in in the development of scarce urban resources [7]. The lower and upper bounds of core aspect ratio are chosen according to the previous wind tunnel investigation of lift-up design [18]. The upper bound of core number is chosen according to the actual row numbers of the lift-up core in the campus university [3], and considering the practical implementation, is set to be six. (iii) The main purpose of this study is to determine the best arrangement of lift-up configuration for optimum wind comfort around the building. Wind comfort is thus the objective, which is evaluated by the normalized index (mean wind velocity ratio). (iv) The specific DOE scheme for the computer experiment should be selected [39]. The BBD is one of most popular

computational experimental designs for formulation of the approximated functions between the response and relevant variables; it has been widely used in optimization designs integrated with CFD simulations [21, 24, 25]. The BBD design has high rotatability, and experimental error is reduced by repeated center points. Moreover, similar studies, such as those by Ng et al. [21] and Shen et al. [24], have demonstrated that the BBD design can achieve high performance in model development while requiring a moderate number of design points. Thus, the BBD design is utilized in this study. (v) After completing the above steps, the design dataset can be generated for DOE.

The second step and the prerequisite for successful implementation of the optimization method is the establishment of reliable CFD simulation for the specific wind flow, which can be guaranteed by rigorously following these steps. (i) A proper turbulence model must be chosen for the CFD simulation, e.g., steady RANS turbulence models, DES or LES. In this study, DES is chosen for the CFD simulation because of its good flow prediction ability for complex wind environments (similar as LES) and its moderate computational cost [15, 33]. (ii) A high-resolution and high-quality mesh system must be constructed for CFD simulation, and a structural grid system is preferred [40, 41]. (iii) The computational settings, which include computational domain, boundary conditions and discretization scheme, must be selected properly according to the best practice guidelines (BPGs) [40, 41]. (iv) Experimental or on-site measurement data should be used to guarantee confident CFD simulation.

The third step of the optimization method is to establish the RSM model. (i) The Meta models, including Standard Response Surface, Kriging, and Neural Network, should be selected. The Standard Response Surface method can establish correlations between the selected design variables and the design objective via implementation of a regression analysis. It is often utilized for optimization purposes for its good performance in complex problems [38]. Moreover, this method has been found to provide satisfactory optimization results in other studies that match very well with this study [21, 23-25]. Thus, the Standard Response Surface is adopted for this study. (ii) The least square method [42] and backward elimination method [43] can be used to generate a first-order and second-order fitted response to evaluate correlations between the design variables. In particular, the backward elimination method should be utilized to eliminate the insignificant term in the fitted RSM model. (iii) The quality and goodness of the fitted RSM model can be examined by analysis of variance (ANOVA). (iv) The fitted RSM model should be verified by additional randomly selected points within the design space.

The last step of the optimization method is to use a proper optimization algorithm to obtain optimum wind comfort. In this study, the Genetic Algorithm (GA) [44] is used for the optimization process by mimicking organic evolution, namely crossover, mutation and selection, on the chromosome of each individual variable. The working principle of the GA to obtain optimal wind comfort is shown in Fig. 3.

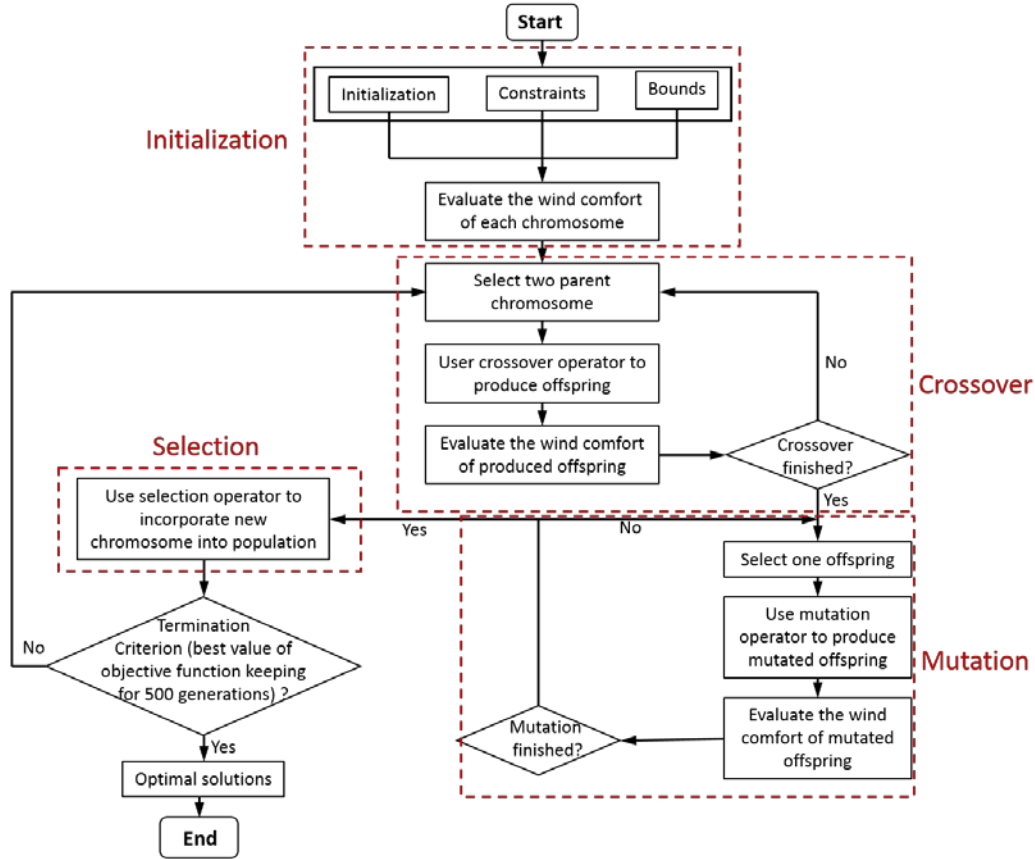


Fig.3. Working principle of the GA to obtain optimum wind comfort.

3. Design parameters

3.1 Description of design variables

The study objective is to determine the lift-up design configuration for optimum wind comfort and the inter-relationship between the influencing variables: the height of lift-up design, $H_L(m)$; the core aspect ratio, $AR(\%)$; and the core number N . The schematic display of the building dimension that have three cores ($N = 3$) is shown in Fig.4, which is adopted from our previous studies [3, 15, 45].

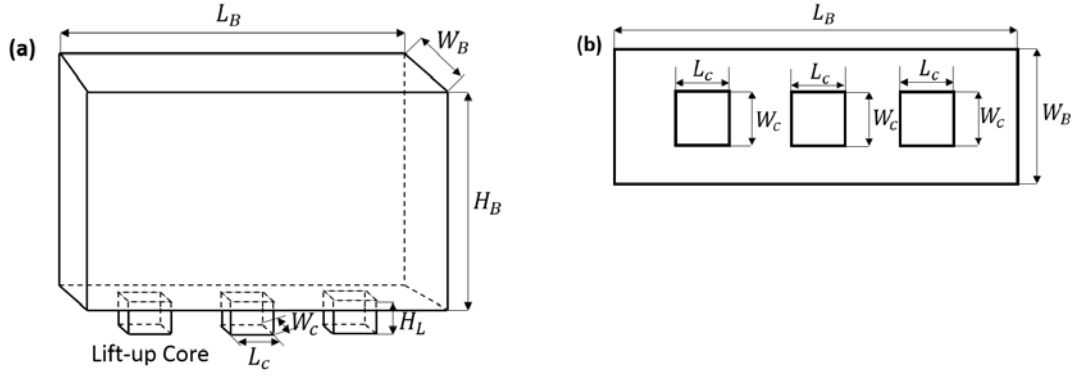


Fig.4. Schematic show of the lift-up design: (a) 3-D view; (b) plan view.

To determine the lift-up design for optimum wind comfort, only the geometric change of lift-up design is considered, and the upper part of the building (building height $H_B(m)$; building length $L_B(m)$ and building width $W_B(m)$) are kept constant during the optimization process. It should be mentioned that the dimensions of building upper part are adopted directly from the previous wind tunnel tests [45], which have been proven to result in the lowest wind speed zones among a number of building designs [56]. The design variables of lift-up building are summarized in Table 1. The range of design variables is explained in Section 2.2. It should be mentioned that because the range of core number is nonconsecutive, the integer part of the calculated value is used to obtain the design value. For example, if the calculated value of N is 3.5, then the design value of N is 3. In particular, the lift-up core arrangements for different numbers (N) under the same core aspect ratio (AR) are schematically shown in Fig.5. Note that the plan configurations of lift-up cores are determined in following order: first, the total size of the lift-up core is calculated based on the core aspect ratio (AR). The individual core size is then obtained from the total size divided by core number (N). The lift-up cores are evenly distributed beneath the building regardless of the configuration. The core aspect ratio is defined with the following equation:

$$AR = \sum_{i=1}^N (L_c \times W_c) / (L_B \times W_B) = N \times L_c \times W_c / (L_B \times W_B) = 3W_c^2 / (L_B \times W_B) \quad (3)$$

here, L_c and W_c are the lift-up core length and core width, respectively.

Table 1. Summary of building design variables

Design variables	Description	Lower limit	Upper limit
$H_L(m)$	Lift-up height	4	8
$AR(\%)$	Lift-up core aspect ratio	10%	70%
N	Lift-up core number	1	6
Design constants		Values	
$H_B(m)$	Building height	50	
$L_B(m)$	Building length	75	
$W_B(m)$	Building width	25	

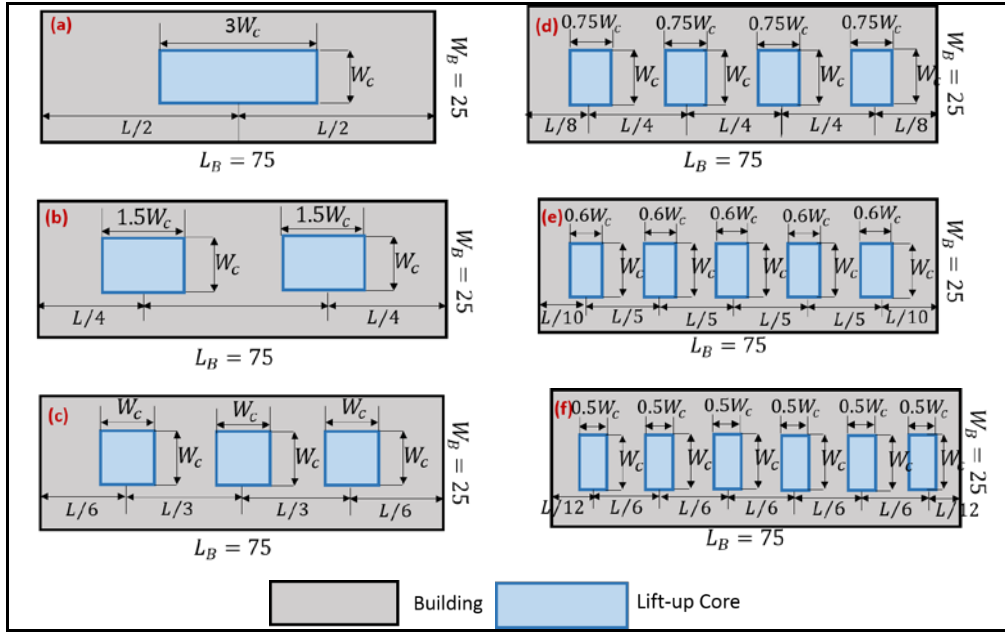


Fig.5. Plan view of lift-up core arrangement for different numbers of : (a) $N = 1$; (b) $N = 2$; (c) $N = 3$; (d) $N = 4$; (e) $N = 5$; (f) $N = 6$.

3.2 Identification of objective parameters

The mean wind velocity ratio (MVR), which is defined as the mean wind velocity at pedestrian level normalized by the mean wind velocity at the reference height, is used in this study to evaluate the wind comfort parameter [3, 8]. The normalized parameter can be described with the following equation:

$$MVR = U_p / U_r \quad (4)$$

here, U_p means the mean wind velocity at pedestrian level at any point of interest; U_r stands for the mean wind velocity at reference height (here, 200m of approach flow).

To assess wind comfort in a quantitative manner, the area-weighted average MVR (\overline{MVR}) is utilized as the objective parameter. It can be described as follows:

$$\overline{MVR} = \int MVR' dA / A \quad (5)$$

where, MVR' is the MVR value at any location at pedestrian level, and A is the area of the target region.

For an isolated building with lift-up design, the lift-up area is defined as the void space formed between the ground and the building above, and the podium area is defined as the neighboring space outside the isolated building, as indicated in Fig. 6. Our previous studies indicate that the wind environment in the lift-up area is quite different from that in the podium area [3, 15, 18]. Thus, for a systematic description of the wind comfort around the building

with lift-up design, the \overline{MVR} is differentiated in the lift-up area and the podium area: \overline{MVR}_L is the \overline{MVR} value in the lift-up area, and \overline{MVR}_P is the \overline{MVR} value in the podium area.

Our previous studies showed that the lift-up design can significantly affect the wind and thermal environment, but only limited to the neighboring area [3, 15]. In particular, the affected areas are mainly within $1H_B$ in upstream region and $2H_B$ in the downstream region when the approaching wind is normal to the building. Thus, the target region for this study is $1H_B$ upstream, $2H_B$ downstream and $1H_B$ lateral from the building as shown in Fig. 6. The podium area thus includes the upstream, downstream and lateral areas in the target region.

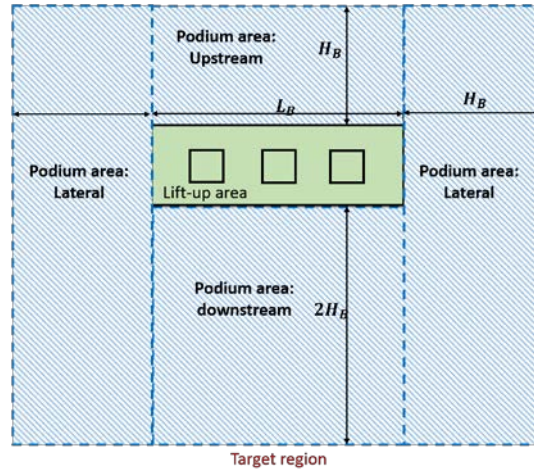


Fig. 6. Target region for evaluation of wind comfort.

3.3 Identification of wind comfort criteria in Hong Kong

The Dutch wind nuisance standard NEN 8100 (2006) has been widely used for assessing wind comfort in recent years [9, 57]. In this criterion, the mean wind velocity of 5 m/s is used as the threshold wind velocity while the probability that exceeds 5 m/s is set as the standard for evaluate different wind comfort level. The wind comfort in Hong Kong will be considered as good for all activity forms when using NEN 8100 for assessment, since the mean wind velocity at reference height (200m) is 5 m/s in Hong Kong [3]. It can be concluded that this wind comfort criterion is incapable for evaluating weak wind conditions of Hong Kong. On the contrary, the new wind comfort criteria proposed by our earlier study [8] aims to evaluate the weak wind condition and the parameters are carefully chosen to adapt the weak wind conditions in high-density Hong Kong. Thus, the new wind comfort criteria proposed in our previous study is adopted in this study.

According to new wind comfort criteria of Hong Kong [8] and AVA scheme [7], the minimum wind velocity to maintain an acceptable wind comfort is 1.5 m/s. Because the mean

wind velocity at the reference height (200m) is 5 m/s in Hong Kong, the wind environment has an acceptable wind comfort when the *MVR* value is equal 0.3 or higher. If the *MVR* value is lower than 0.3, the wind environment is deemed unacceptable. Because a higher wind velocity is generally preferred in Hong Kong, a greater *MVR* value will be considered to result in greater wind comfort [3]. However, when the wind velocity exceeds 5.3 m/s, wind comfort becomes poor due to the strong mechanical force caused by the strong wind [8]. Thus, wind comfort is acceptable with in a *MVR* value range of 0.3 to 1.06, and a larger value means better wind comfort in this study.

4. CFD validation

4.1 Turbulence model

The detached-eddy simulation (DES) model, which is a well-known hybrid RANS and LES approach [46], is selected here to reproduce the wind flow at pedestrian level. Because it can produce similar prediction results for the wind flow around an isolated building at a lower computational cost than LES [33, 35]. During the CFD simulation, the flow is treated as an incompressible Newtonian fluid and the air density change due to solar heating of stagnant air is not considered in this study. For an isothermal turbulent incompressible flow, the governing equations of mass and momentum can be described as follows:

$$\partial \bar{u}_i / \partial x_i = 0 \quad (6)$$

$$\frac{\partial \bar{u}_i}{\partial t} + \frac{\partial \bar{u}_i \bar{u}_j}{\partial x_j} = \frac{1}{\rho} \left(\frac{\partial}{\partial x_j} \left(\nu \frac{\partial \bar{u}_i}{\partial x_j} \right) - \frac{\partial \bar{P}}{\partial x_i} - \frac{\partial \tau_{ij}}{\partial x_j} \right) \quad (7)$$

here, the overbars indicate the filtering operator; t is the time; u_i and u_j are the velocity component; ρ is the density, and for incompressible assumption here, $\rho = 1$; ν stands for viscosity; P represents the pressure; τ_{ij} is the sub-grid scale (SGS) stress term that arisen by turbulence model and is defined by Equation (8).

$$\tau_{ij} \equiv 1/\rho (\overline{u_i u_j} - \bar{u}_i \bar{u}_j) \quad (8)$$

The DES modelling approach is based on the one equation Spalart-Allmaras (S-A) eddy viscosity model, which provides solution of a modelled transport equation for the turbulent viscosity variable ($\tilde{\nu}$) [47]. The description of the S-A eddy viscosity model is as follows:

$$\frac{\partial \tilde{\nu}}{\partial t} + \frac{\partial}{\partial x_i} (\tilde{\nu} u_i) = C_{D1} \tilde{S}_\nu \tilde{\nu} + \frac{1}{\sigma_\nu} \{ \nabla \cdot [(\nu + \tilde{\nu}) \nabla \tilde{\nu}] + C_{D2} (\nabla \tilde{\nu})^2 \} - c_w f_w \left[\frac{\tilde{\nu}}{d} \right]^2 \quad (9)$$

In Equation (9), the left-hand side contains a local change term and a convective term; and the right-hand side includes a production term, a diffusion term and a destruction term. The

related constants are $C_{D1} = 0.1355$, $\sigma_v = 2/3$, $C_{D2} = 0.622$, $c_w = 0.1355/k^2 + 2.433$. f_w is wall destruction function. d is the distance from the first node to the wall surface. The relationship between the new eddy viscosity variable ($\tilde{\nu}$) and the eddy viscosity variable (μ_t) can be described by Equation (10).

$$\mu_t = \tilde{\nu} f_{v1}, f_{v1} = \frac{\chi^3}{\chi^3 + C_v^3}, \chi \equiv \frac{\tilde{\nu}}{\nu} \quad (10)$$

here, C_v is a constant, which equals to 7.1; and f_{v1} and χ are intermediate variables. In the hybrid DES modelling approach, the RANS mode is used in the boundary layer and the LES mode is activated in the flow separation area. Moreover, the above standard formulation of the S-A model, which is defined by Equation (9), is modified into an unsteady mode by DES treatment and the length scale d is revised by a new parameter \tilde{d} as follows:

$$\tilde{d} = \min(d, C_{DES} \Delta_{max}) \quad (11)$$

here, the filter spacing Δ_{max} is the largest grid spacing in the x, y, or z directions ($\Delta_{max} = \max(\Delta x, \Delta y, \Delta z)$). The empirical constant C_{DES} is 0.65 [48]. The revised parameter \tilde{d} guarantees the switching process of the DES treatment between RANS and LES modes. When $d > \Delta_{max}$, the LES mode is active; otherwise, the RANS mode is used. Notably, inaccurate prediction results will occur during DES modelling if the LES mode is used in insufficient fine boundary layers and shallow separation regions. Thus, Spalart et al. [49] revised the standard DES modelling approach into Delayed DES model by re-defining the DES length scale \tilde{d} , which ensures that the RANS mode is used throughout the boundary layer. The DES length scale of \tilde{d} is redefined by:

$$\tilde{d} = d - f_d \max(0, d - C_{DES} \Delta_{max}) \quad (12)$$

$$f_d \equiv 1 - \tanh([8R_d]^3), R_d \equiv \frac{\nu_t + \nu}{\kappa^2 d^2 \sqrt{U_{i,j} U_{i,j}}} \quad (13)$$

where, ν_t is kinematic eddy viscosity and ν stands for molecular viscosity. κ is the Karman constant with a value of 0.41 and $U_{i,j}$ are velocity gradients; f_d and R_d are intermediate variables.

Based on the above discussion and recommendations from the literature [15, 33, 50], the Delayed DES model is selected for this study to simulate the pedestrian level wind environment.

4.2 Building description

The experimental data from the wind tunnel tests conducted by Xia et al. [45] in regards to the wind flow around an isolated building with lift-up design were employed in this study for

validation purpose, which were carried out in the high-speed of the CLP power wind/wave tunnel facility at the Hong Kong University of Science and Technology. The building geometry and dimensions are the same as the schematic diagram shown in Fig.7, in which three structural pillars were used to “lift” the building. The building dimensions are $50\text{m}(H_B) \times 75\text{m}(L_B) \times 25\text{m}(W_B)$, and those of the three pillars are $8\text{m}(D) \times 8\text{m}(d) \times 3.5\text{m}(H_L)$. The arrangement of pillars are the same as that presented in Fig. 5(c). The building with lift-up design was constructed on a geometric scale of 1:200, and this scale is also adopted for all CFD simulations in this study. The wind profile followed the form of power law with the exponent of 0.2 ($U(z)/U_r = (Z/Z_r)^{0.2}$) with the mean wind velocity (U_r) of 10m/s at the reference height (150m in prototype scale; 0.75m in model scale). The inflow wind profile ($U(z)$) and the turbulence intensity ($I(z)$) for the wind tunnel tests and CFD simulation are presented in Fig.7 (a). It should be mentioned that the similarity requirements were carefully checked during the wind tunnel tests with a Reynolds number of 8.2×10^4 at the reference building height, which guaranteed the Reynolds number independence during the tests. More detailed information on the wind tunnel tests can be found in the literatures [3, 15, 45].

4.3 Boundary conditions and numerical details

The description of the computational domain and boundary conditions are presented in Fig.7 (b), which comply with the recommendations of the best practice guidelines (BPGs) for CFD simulations [40, 41]. The resulting blockage ratio is only 1.04%, which is far lower than recommended limit value of 3% [40,41]. It should be noted that structural hexahedral grids were used to discretize the entire computational domain. The quality of the grids is very high, which can be seen in Fig. 11, and at least five cells have been placed at pedestrian level as suggested by the BPGs [40, 41]. As for RANS model setting of the Delayed DES model, the realizable $k - \varepsilon$ is used in this study. The pressure and momentum equations were coupled by utilizing the PISO algorithm, and the bounded central differencing and second-order upwind scheme were used for the convective term and the diffusion term, respectively. The residuals of all the calculations were set at 10^{-5} during the simulation.

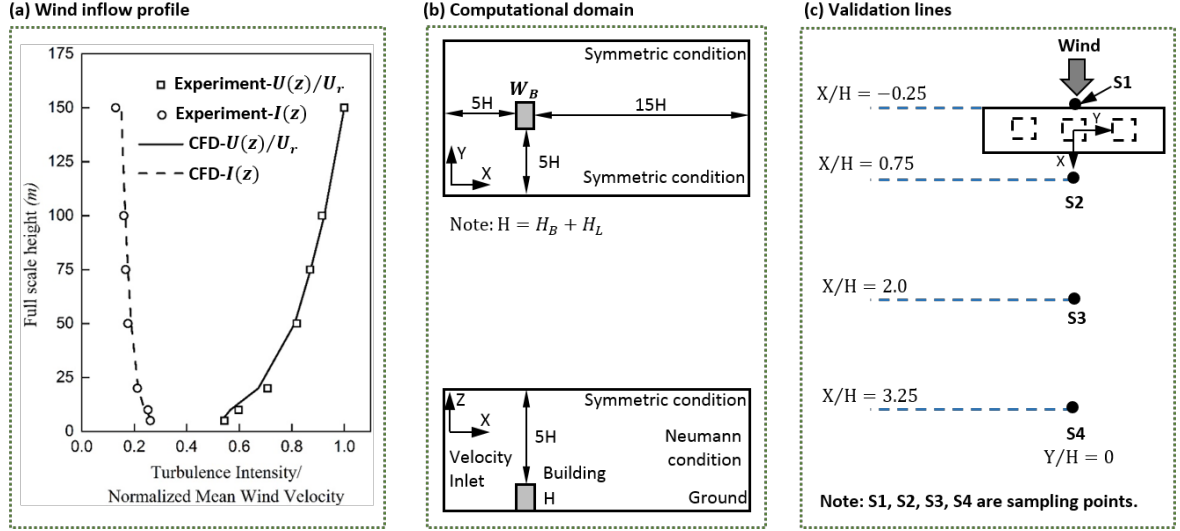


Fig. 7. Boundary conditions and validation lines: (a) Wind inflow profile of the normalized mean wind velocity and turbulence intensity; (b) Computational domain of the CFD simulation; (c) Validation lines at the pedestrian level ($Z/H = 0.04$).

4.4 Sensitivity test

As indicated by previous studies of transient turbulence models [15, 16, 37, 50], three important computational parameters should be tested during the sensitivity test process, namely grid size, discretization time step and sampling time. Based on previous studies by Liu and Niu [15, 16, 33], the discretization time steps (Δt) of 0.01, 0.005 and 0.001 s were tested to obtain the independence of Δt . Moreover, the non-dimensional sampling time unit t^* , which is defined as $t^* = t \times \langle U_H \rangle / H$, is utilized to represent the length of sampling time. Three values of t^* (320, 416, and 480) were selected to determine the independence of t^* , which correspond with real periods (t) of 10, 13 and 15 s. The independence test results of some important computational parameters for the DES model are summarized in Table 2, which includes various minimum grid sizes, time step sizes and sampling times. Table 2 also shows that DES-1, DES-2, and DES-3 are used for grid sensitivity test; DES-2, DES-4, and DES-5 for time step sensitivity test; DES-2, DES-6 and DES-7 for sensitivity test of sampling time.

Table 2. Different arrangements of computational parameters

Case	Min grid size (m)	Δt (s)	t^*
DES-1	0.001	0.005	320
DES-2	0.0005	0.005	320
DES-3	0.00025	0.005	320
DES-4	0.0005	0.01	320
DES-5	0.0005	0.001	320
DES-6	0.0005	0.005	416
DES-7	0.0005	0.005	480

Fig. 8 presents the results of the sensitivity test in the line of $X/H = 0.75$ at pedestrian level. Three grid systems are constructed for grid sensitivity test (see Fig. 9), with minimum grid sizes of 0.001, 0.0005 and 0.00025 m. The corresponding numbers of cells for these grid systems are 2.9 million, 4.1 million, and 5.9 million, respectively. Fig.8 (a) shows that the results given by DES-2 and DES-3 are nearly the same, whereas those of DES-1 show large discrepancies, which suggests that the minimum grid size of 0.0005 m is sufficiently fine for the DES simulation. For the time step sensitivity test, Fig. 8 (b) illustrates that DES-3 and DES-5 have the similar prediction results, whereas DES-4 shows evident differences from the others, which suggests that Δt of 0.005 s is sufficient to model the wind environment around the building. Meanwhile, the comparison results in Fig. 8(c) are almost the same for DES-3, DES-6 and DES-7. Thus, taking into consideration the simulation accuracy and computational costs, the computational parameters used in DES-3 are sufficient to model pedestrian level wind environment in this study.

(a) (b) (c)
Fig. 8 Sensitivity test results for the DES model: (a) grid sensitivity test; (b) time step sensitivity test; (c) sampling time sensitivity test.

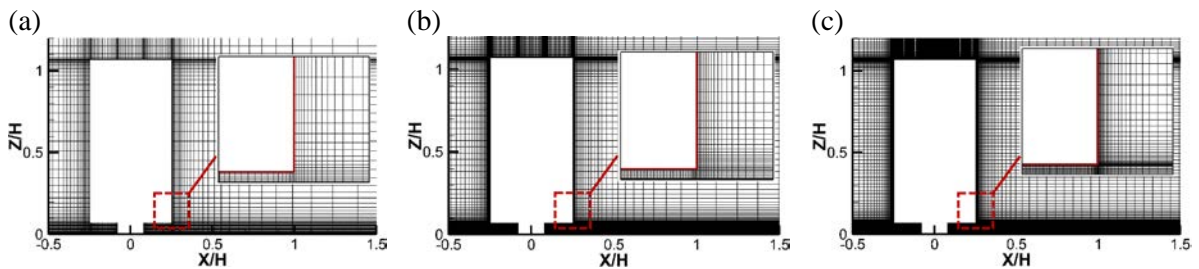


Fig. 9 Mesh information on vertical plan of $Y/H = 0$: minimum grid sizes of (a) 0.001 m; (b) 0.0005 m; (c) 0.00025 m.

4.5 Validation results

The validation lines at pedestrian level for which the experimental data and the simulation results are compared are shown schematically in Fig. 7(c). Four points (S1, S2, S3, and S4) are chosen to present the time history of the sampling wind velocity U . It should be mentioned that

the mean wind velocities are used for validation purposes. Moreover, the validation of these wind tunnel tests was presented in our earlier study [3]. The numerical methods and boundary conditions were also described in detail in our earlier study [3]. In particular, the Renormalizations Group (RNG) $k - \varepsilon$ model was used in the earlier validation. Fig. 10 presents the comparison results between these CFD models against the experimental data. As shown in Fig. 10, the DES model and the RANS model both generally agree with the wind tunnel test results, especially at the windward side. However, the DES model presents better prediction results than the RANS model (RNG $k - \varepsilon$ model) at the leeward side of the building. Thus, DES model can reproduce the wind flow at pedestrian level better than that of RANS model. Even though the prediction results slightly overestimate the wind velocity at some points, the validation results indicate that the DES model can be utilized to simulate the wind flow at pedestrian level around the building with lift-up design. In addition to the validation results, the fluctuation characteristic of four sampling points, which are on the center line of the building as indicated in Fig.7 (c), are also presented here. Fig. 11 shows the time history of *MVR* values for the four sampling points. The fluctuations of Point S1 and Point S2 are more evident than those of Point S3 and Point S4, which means that the LES model is active in the regions of Point S1 and Point S2, whereas the RANS model is active in the regions around Point S3 and Point S4. Because Point S3 and Point S4 are farther from the building than Point S1 and Point S2, and the relevant mesh density is coarser in regions away from the building than in those near the building. From these results, it can be argued that the DES modelling technique is a good choice for prediction of the pedestrian level wind environment around an isolated building with lift-up design.

(a) (b) (c) (d)

Fig.10 Comparison of *MVR* results between CFD simulations and experimental data: (a) $X/H = -0.25$; (b) $X/H = 0.75$; (c) $X/H = -2.0$; (d) $X/H = 3.25$.

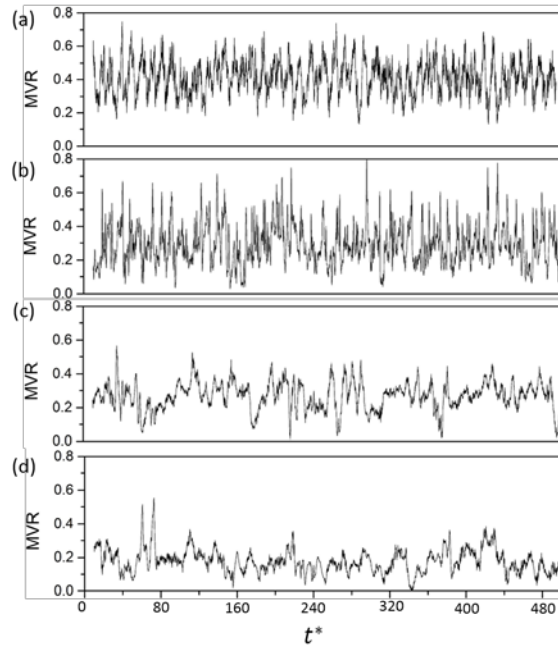


Fig.11 Time history of monitored MVR values at four sampling points: (a) Point S1; (b) Point S2; (c) Point S3; (d) Point S4.

5. Results and discussion

5.1 Development of response surface model

In this study, the BBD is utilized as the DOE scheme, and the software of Design Experts software is used for experimental design. The dataset generated by BBD design and the results obtained from CFD simulation are listed in Table 3. It should be mentioned that the center design point is repeated several times during the CFD simulations.

Table 3. BBD-based design dataset and obtained CFD results

Design points			\overline{MVR}_L	\overline{MVR}_P
$H_L(m)$	$AR(\%)$	N		
6	40	3	0.403	0.473
4	40	6	0.469	0.450
6	10	1	0.512	0.473
8	40	1	0.371	0.469
4	70	3	0.355	0.446
6	10	6	0.607	0.505
8	70	3	0.361	0.451
4	40	1	0.365	0.450
8	40	6	0.468	0.451
6	70	1	0.340	0.461
6	70	6	0.420	0.439
4	10	3	0.521	0.469
8	10	3	0.530	0.482

After performing the CFD simulations listed in Table 3, the obtained results are used to determine the RSM models in the lift-up area and podium area. The Linear (first-order) and Quadratic (second-order) models of Eq. (2) are used to obtain the coefficients of the model. The backward regression method is utilized to eliminate the insignificant terms of the model. The established RSM models for prediction of \overline{MVR}_L and \overline{MVR}_P are shown in Table 4 and Table 5, respectively. Moreover, the regression analysis parameters of Predicted R^2 and Adjusted R^2 are employed to indicate the goodness of the response models to predict the responding values. The closer the R^2 values are to one, the greater the predictive ability of the response models. Noted that Adjusted R^2 is a modification of Predicted R^2 , which adjusts for the number of explanatory terms. It can be seen from Table 4 and Table 5 that the Linear (first-order) formulated models are not suitable for fitting the models for \overline{MVR}_L and \overline{MVR}_P , whereas the Quadratic (second-order) formulated models are in good agreement with the obtained values \overline{MVR}_L and \overline{MVR}_P with CFD simulation results. Therefore, the RSM models of Quadratic (Second-order) approximations are adopted in this study. Meanwhile, the Quadratic approximations that the established models contain the terms $H_L \times N$ and $AR \times N$, which indicates the interactive effect of the design variables.

Table 4 Established RSM models for predicting \overline{MVR}_L

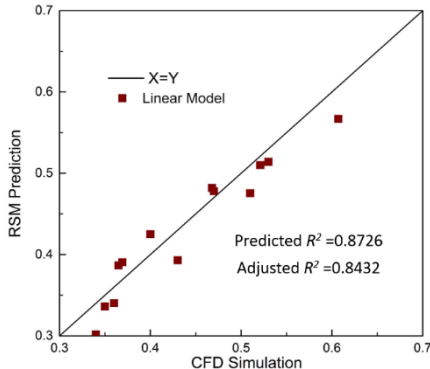
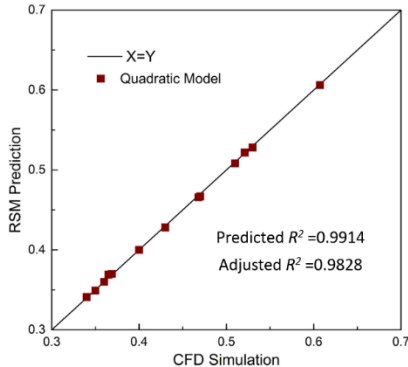
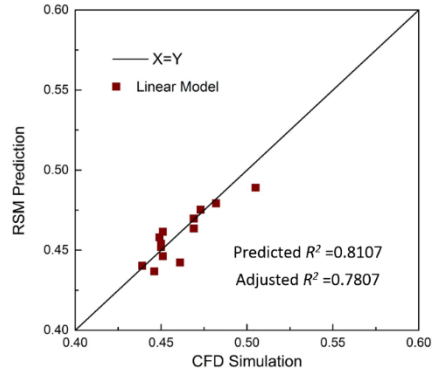
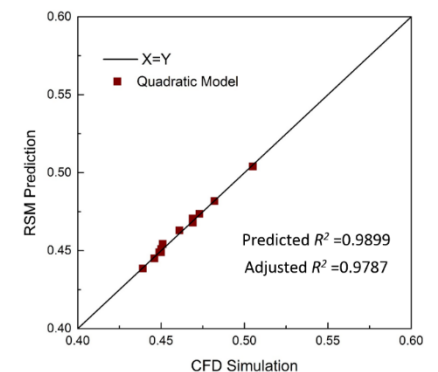
RSM model	RSM vs. simulation plot
<p>Linear (first-order) model</p> $\overline{MVR}_L = 0.48 + 0.001H_L - 0.29AR + 0.018N$	
<p>Quadratic (second-order) model</p> $\overline{MVR}_L = 0.547 + 0.003H_L - 0.651AR + 2.07 \times 10^{-3}N - 2 \times 10^{-4}H_L \times N - 4.33 \times 10^{-3}AR \times N + 0.489AR^2 + 2.73 \times 10^{-3}N^2$	

Table 5. Established RSM models for predicting \overline{MVR}_p

RSM model	RSM vs. simulation plot
<p>Linear (first-order) model</p> $\overline{MVR}_p = 0.467 + 2.375 \times 10^{-3}H_L - 0.055AR + 4 \times 10^{-4}N$	
<p>Quadratic (second-order) model</p> $\overline{MVR}_p = 0.453 + 5.53 \times 10^{-3}H_L - 0.122AR + 3.62 \times 10^{-3}N - 9 \times 10^{-4}H_L \times N - 0.018AR \times N + 0.163AR^2 + 1.23 \times 10^{-3}N^2$	

The adequacy of the RSM models established above are verified by analysis of variance (ANOVA), and checked at the 95% confidence level. Table 6 shows the results from the ANOVA analysis of the established RSM models. The p-values for regressions are below 0.0001 (with F-ratio values over 50), which means that the regression models are significant and good to fit. Moreover, the p-values for Lack-of-fit tests are over 0.2 (>0.05), which implies that the quadratic models are adequate for this study.

Table 6. Analysis of variance (ANOVA) for established RSM models

	Variation source	F-ratio	P-value	Significance
Quadratic model for \overline{MVR}_L	Regression	67.57	<0.0001	Significant
	Lack-of-fit	1.84	0.2852	Not significant
Quadratic model for \overline{MVR}_p	Regression	52.44	<0.0001	Significant
	Lack-of-fit	2.30	0.2195	Not significant

5.2 Verification of RSM models

To verify the RSM models established in Section 5.1, four random datasets within the design space are selected. Table 7 summarizes the detailed information of the dataset and verification results, and compares the values predicted by CFD and the established RSM model. It can be concluded that the established RSM models show good agreement with the CFD simulation results, which in turn proves the goodness of fit of the established models for this study.

Table 7. Validation dataset for established RSM models

Design Points			\overline{MVR}_L		\overline{MVR}_p	
$H_L(m)$	$AR(\%)$	N	CFD	RSM	CFD	RSM
5	20	2	0.466	0.460	0.465	0.459
5	60	4	0.374	0.377	0.434	0.439
7	30	2	0.429	0.420	0.467	0.468
7	50	5	0.418	0.416	0.450	0.453

5.3 Correlation of parameters

The influences of each design variable on the respondent values of \overline{MVR}_L and \overline{MVR}_p are investigated by conducting the Parameters Correlation analysis [51]. The Spearman's rank correlation method is employed to ascribe the degree between the design variables and the relevant output values. To use the Spearman's rank correlation method, 90 unique and random data sets are generated via the Latin Hypercube Sampling methods, which considers 5% deviation of correlations [51]. The estimated correlation values between the three design variables and the respondent values are summarized in Table 8. The correlation values between lift-up aspect ratio (AR) and the respondent values are negative, which means that the values of \overline{MVR}_L and \overline{MVR}_p will benefit from the decrease of lift-up blockage. In addition, the absolute correlation values of AR are largest both for \overline{MVR}_L and \overline{MVR}_p among the three design variables, as shown in Table 8, which suggests that the lift-up aspect ratio is the most influential design variable for evaluation of \overline{MVR}_L and \overline{MVR}_p . However, for the other two design variables, the lift-up core number is the second most influential design variable when evaluating \overline{MVR}_L and the lift-up height is the second most influential design variable when evaluating \overline{MVR}_p .

The correlations between the design variables are also examined in this study and are presented in Table 8. The absolute values of correlation are around zero, which indicates little relevance between these design variables. Thus, it is safe to say that no strong relationship exists between the selected variables in this study.

	H_L	AR	N	\overline{MVR}_L	\overline{MVR}_P
H_L	1.0	0.358	0.0	0.0	0.0
AR	0.358	1.0	-0.877	0.0	0.0
N	0.0	-0.877	1.0	0.586	0.0
\overline{MVR}_L	0.0	0.0	0.586	1.0	0.436
\overline{MVR}_P	0.0	0.0	0.0	0.436	1.0

To improve the pedestrian level wind comfort, the commonly used GA optimization method is used to obtain the optimum wind comfort around an isolated building with lift-up design. Because the priority of the paper is to find the design variables for the optimum wind comfort, as well as the space of the paper is limited, detailed information on GA can be found in literature [52-54].

To verify the optimized \overline{MVR}_L and \overline{MVR}_P values predicted by the RSM models, CFD simulation is conducted again with the design variables obtained above. The simulated results for \overline{MVR}_L and \overline{MVR}_P are 0.719 and 0.502, respectively, which agrees well with those predicted with the RSM models. Thus, it can be concluded that the best design point is that H_L is 8m, AR is 10% and N is 6.

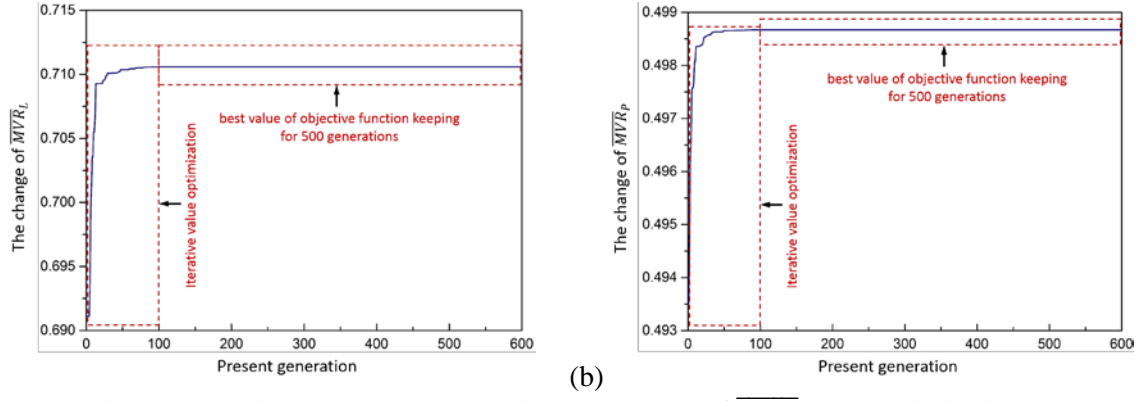


Fig.12 Iterative computation process: (a) Optimization process of \overline{MVR}_L ; (b) Optimization process of \overline{MVR}_P .

5.5 Optimum pedestrian level wind comfort

The obtained initial (validation case) and best (optimal case) pedestrian level wind environments are presented in Fig.13. In general, the wind environment at pedestrian level is improved by the optimization method, especially in the upstream near-field low wind velocity zone, the lift-up high wind velocity zone and the downstream near-field wind velocity zone. As indicated in Section 3.3, the wind environment has acceptable wind comfort when the MVR value is between 0.3 and 1.06, and a higher value of MVR indicates greater wind comfort [3]. The wind comfort in upstream area in Fig.13 (a) is unacceptable, whereas the wind comfort in the upstream area in Fig.13 (b) is acceptable. Besides, a large portion of the lift-up area has unacceptable wind comfort, especially behind the lift-up cores (see Fig. 13 (a)). However, Fig. 13 (b) shows that the unacceptable wind comfort is reduced significantly after the optimization process. Furthermore, the wind comfort of the leeward side near the building is much better in Fig. 13 (b) than in Fig. 13 (a). It should be noted that if the MVR value is over 1.06, the wind comfort becomes unacceptable [8], and strong wind conditions may be dangerous to pedestrians. However, there is no such high wind velocity zone that causes wind nuisance to pedestrians in Fig. 13. Therefore, it can be concluded from the above information that the proposed optimization method can effectively improve the wind comfort at pedestrian level around an isolated building with lift-up design.

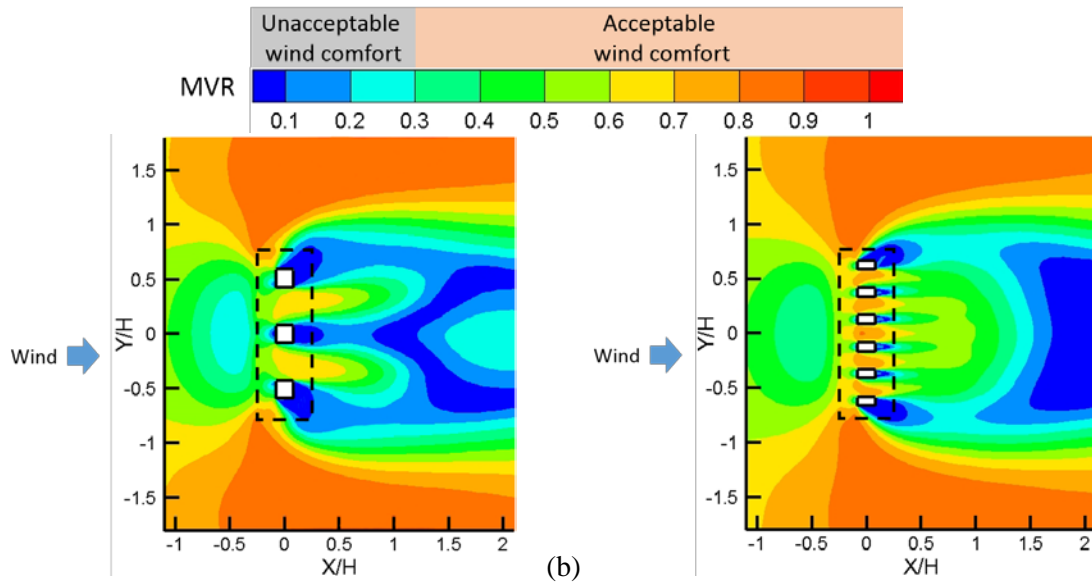


Fig. 13. Comparison results of pedestrian level wind environment: (a) validation case; (b) optimal case.

5.6 Discussion

This investigation intends to provide a generalized study to determine the optimum wind comfort around an isolated building with lift-up design by using the proposed multi-variable optimization method. Only one type of building dimension is considered in this paper. However, the building dimensions have been identified to have influence on pedestrian level wind environment in the previous study [56]. Further studies are still needed to fully apply the results to building with different dimensions.

In this study, the combination of the RSM meta-model with CFD simulation results successfully predicts the relationship between the lift-up design variables and wind comfort. Moreover, the optimum wind comfort around the building is determined. In particular, the utilization of BBD method is proven to perform well during the optimization process. However, other DOE methods, including CCD, OPD and FFD methods, have also been found to be reliable during optimization process [19,21,23, 25, 55]. Thus, comprehensive investigations of the influence of various DOE methods on optimized results can be carried out in the future study.

It has been identified that the approaching wind direction can affect the wind flow field around the building [3]. Thus, further investigations are still required to study the optimal results under different approaching wind directions. In addition, the local wind statistics should be considered in actual application of the proposed multi-variable optimization method.

6. Conclusions

This study focuses on determination of the optimum lift-up design parameters for optimal wind comfort around an isolated building with lift-up design. An integrated computational optimization method is proposed that combines the RSM meta-model with CFD simulation results. Considering the computational costs and prediction accuracy, the DES modelling technique is employed to complete the CFD simulations. Three design variables are varied simultaneously during the optimization process: lift-up height (H_L), lift-up core aspect ratio (AR) and lift-up core number (N). After following the optimization method, the relationships between the design variables and wind comfort are established. The adequacy of the models is analyzed by ANOVA and the models are verified by comparing obtained results with four randomly selected datasets. In addition, the GA optimization method is utilized to obtain the optimum wind comfort from the established RSM model.

The main findings of the study are summarized as follows: (i) within the range of design variables, an H_L of 8 m, an AR of 10%, and an N of 6 produce the best response results for both \overline{MVR}_L and \overline{MVR}_p . (ii) The lift-up design variables influence the wind comfort on a different level. (iii) The lift-up aspect ratio is the most influential parameter for evaluation of \overline{MVR}_L and \overline{MVR}_p . Moreover, the lift-up core number is the second most influential parameter when evaluating \overline{MVR}_L , whereas the lift-up height prevails over the lift-up core number when evaluating \overline{MVR}_p .

In general, the results clearly demonstrate that the proposed multi-variable optimization method can be successfully used to obtain parameters for optimum wind comfort around an isolated building with lift-up design. The correlation between the design variables and wind comfort can also be obtained from this method. Furthermore, this study serves as a good demonstration of the application of the optimization method that can also be used in similar studies. For practical design, the core aspect ratio should be low and the lift-up design should have multiple cores. Moreover, the lift-up core aspect ratio should assume a higher priority than the other two design variables when constructing the lift-up design. The outcomes of this study can also be of value to improve wind comfort in high-rise cities such as, Hong Kong.

Acknowledgement

The work described in this paper was fully supported by a grant from the Research Grants Council of the Hong Kong Special Administrative Region, China (Project No. C5002-14G). Special thanks are given to Mr. Jianlin LIU for the suggestions on CFD simulation.

References

- [1] J.L. Niu, J.L. Liu, T.-C. Lee, Z. Lin, C. M. Mak, K.-T. Tse, B.-S. Tang, K.C.S. Kwok, A new method to assess spatial variations of outdoor thermal comfort: onsite monitoring results and implications for precinct planning, *Build. Environ.* 91 (2015) 263-270.
- [2] Y.X. Du, C.M. Mak, T.Y. Huang, J.L. Niu, Towards an integrated method to assess effects of lift-up design on outdoor thermal comfort in Hong Kong, *Build. Environ.* 125 (2017) 261-272.
- [3] Y.X. Du, C.M. Mak, J.L. Liu, Q. Xia, J.L. Niu, K.C. Kwok, Effects of lift-up design on pedestrian level wind comfort in different building configurations under three wind directions, *Build. Environ.* 117 (2017) 84-99.
- [4] T. Chetwittayachan, D. Shimazaki, K. Yamamoto, A comparison of temporal variation of particle-bound polycyclic aromatic hydrocarbons (pPAHs) concentration in different urban environments: Tokyo, Japan, and Bangkok, Thailand, *Atmos. Environ.* 36 (2002) 2027-2037.
- [5] Z.T. Ai, C.M. Mak, From street canyon microclimate to indoor environmental quality in naturally ventilated urban buildings: Issues and possibilities for improvement, *Build. Environ.* 94 (2015) 489-503.
- [6] J. Hang, Y. Li, Ventilation strategy and air change rates in idealized high-rise compact urban areas, *Build. Environ.* 45 (2010) 2754-2767.
- [7] E. Ng, Policies and technical guidelines for urban planning of high-density cities—air ventilation assessment (AVA) of Hong Kong, *Build. Environ.* 44 (2009) 1478-1488.
- [8] Y.X. Du, C.M. Mak, K.C.S. Kwok, K.-T. Tse, T.-C. Lee, Z.T. Ai, J.L. Liu, J.L. Niu, New criteria for assessing low wind environment at pedestrian level in Hong Kong, *Build. Environ.* 123 (2017) 23-36.
- [9] W. Janssen, B. Blocken, T. van Hooff, Pedestrian wind comfort around buildings: Comparison of wind comfort criteria based on whole-flow field data for a complex case study, *Build. Environ.* 59 (2013) 547-562.
- [10] T. Kubota, M. Miura, Y. Tominaga, A. Mochida, Wind tunnel tests on the relationship between building density and pedestrian-level wind velocity: Development of guidelines for realizing acceptable wind environment in residential neighborhoods, *Build. Environ.* 43 (2008) 1699-1708.
- [11] T. Stathopoulos, R. Storms, Wind environmental conditions in passages between buildings, *J. Wind Eng. Ind. Aerod.* 24 (1986) 19-31.
- [12] Y. -H. Juan, A. -S. Yang, C. -Y. Wen, Y. T. Lee, P. C. Wang, Optimization procedures for enhancement of city breathability using arcade design in a realistic high-rise urban area. *Build. Environ.* 121 (2017) 247-261.
- [13] C.-Y. Wen, Y.-H. Juan, A.-S. Yang, Enhancement of city breathability with half open spaces in ideal urban street canyons, *Build. Environ.* 112 (2017) 322-336.
- [14] A.T. Chan, W.T. Au, E.S. So, Strategic guidelines for street canyon geometry to achieve sustainable street air quality—part II: multiple canopies and canyons, *Atmos. Environ.* 37 (2003) 2761-2772.
- [15] J.L. Liu, J.L. Niu, Q. Xia, Combining measured thermal parameters and simulated wind velocity to predict outdoor thermal comfort, *Build. Environ.* 105 (2016) 185-197.
- [16] J.L. Liu, J.L. Niu, C.M. Mak, Q. Xia, Detached eddy simulation of pedestrian-level wind and gust around an elevated building, *Build. Environ.* 125 (2017) 168-179.
- [17] T.Y. Huang, J.N. Li, Y.X. Xie, J.L. Niu, C.M. Mak, Outdoor thermal comfort study in the underneath-elevated-building (UEB) area: On-site measurements and surveys in Hong Kong, *Build. Environ.* 125 (2017) 502-514.
- [18] K.-T. Tse, X.L. Zhang, A.U. Weerasuriya, S.W. Li, K.C.S. Kwok, C.M. Mak, J.L. Niu, Adopting 'lift-up' building design to improve the surrounding pedestrian-level wind environment, *Build. Environ.* 117 (2017) 154-165.
- [19] T.W. Simpson, J. Poplinski, P.N. Koch, J.K. Allen, Metamodels for computer-based engineering design: survey and recommendations, *Eng. Comput.* 17 (2001) 129-150.
- [20] H. Hotelling, Experimental determination of the maximum of a function, *Ann. of Math. Stat.* 12 (1941) 20-45.
- [21] K.C. Ng, K. Kadirgama, E.Y.K. Ng, Response surface models for CFD predictions of air diffusion performance index in a displacement ventilated office, *Energy Build.* 40(5) (2008) 774-781.

- [22] T. Norton, J. Grant, R. Fallon, D.-W. Sun, Optimising the ventilation configuration of naturally ventilated livestock buildings for improved indoor environmental homogeneity, *Build. Environ.* 45(4) (2010) 983-995.
- [23] X. Shen, G. Zhang, B. Bjerg, Investigation of response surface methodology for modelling ventilation rate of a naturally ventilated building, *Build. Environ.* 54 (2012) 174-185.
- [24] X. Shen, G. Zhang, B. Bjerg, Assessments of experimental designs in response surface modelling process: Estimating ventilation rate in naturally ventilated livestock buildings, *Energy Build.* 62 (2013) 570-580.
- [25] P. Sofotasiou, J.K. Calautit, B.R. Hughes, D. O'Connor, Towards an integrated computational method to determine internal spaces for optimum environmental conditions, *Comput. Fluids* 127 (2016) 146-160.
- [26] B. Blocken, 50 years of computational wind engineering: past, present and future, *J. Wind Eng. Ind. Aerod.* 129 (2014) 69-102.
- [27] A. Mochida, I.Y. Lun, Prediction of wind environment and thermal comfort at pedestrian level in urban area, *J. Wind Eng. Ind. Aerod.* 96(10) (2008) 1498-1527.
- [28] Z.T. Ai, C. M. Mak, CFD simulation of flow and dispersion around an isolated building: Effect of inhomogeneous ABL and near-wall treatment, *Atmos. Environ.* 77 (2013) 568-578.
- [29] B. Blocken, T. Stathopoulos, J. Van Beeck, Pedestrian-level wind conditions around buildings: Review of wind-tunnel and CFD techniques and their accuracy for wind comfort assessment, *Build. Environ.* 100 (2016) 50-81.
- [30] Y. Tominaga, T. Stathopoulos, Numerical simulation of dispersion around an isolated cubic building: model evaluation of RANS and LES, *Build. Environ.* 45(10) (2010) 2231-2239.
- [31] Z.T. Ai, C. M. Mak, J.L. Niu, Numerical investigation of wind-induced airflow and interunit dispersion characteristics in multistory residential buildings, *Indoor air* 23(5) (2013) 417-429.
- [32] D.J. Cui, C.M. Mak, K.C.S. Kwok, Z.T. Ai, CFD simulation of the effect of an upstream building on the inter-unit dispersion in a multi-story building in two wind directions, *J. Wind Eng. Ind. Aerod.* 150 (2016) 31-41.
- [33] J.L. Liu, J.L. Niu, CFD simulation of the wind environment around an isolated high-rise building: An evaluation of SRANS, LES and DES models, *Build. Environ.* 96 (2016) 91-106.
- [34] P. Spalart, W. Jou, M. Strelets, S. Allmaras, Comments on the feasibility of LES for wings, and on a hybrid RANS/LES approach, *Advances in DNS/LES* 1 (1997) 4-8.
- [35] M. Lateb, C. Masson, T. Stathopoulos, C. Bédard, Simulation of near-field dispersion of pollutants using detached-eddy simulation, *Comput. Fluids* 100 (2014) 308-320.
- [36] K.E. Kakosimos, M.J. Assael, Application of Detached Eddy Simulation to neighbourhood scale gases atmospheric dispersion modelling, *J. Hazard Mater.* 261 (2013) 653-68.
- [37] Y. Wu, J.L. Niu, Numerical study of inter-building dispersion in residential environments: Prediction methods evaluation and infectious risk assessment, *Build. Environ.* 115 (2017) 199-214.
- [38] R. H. Myers, D. C. Montgomery, C. M. Anderson-Cook. *Response surface methodology: process and product optimization using designed experiments*[M]. John Wiley & Sons, 2016.
- [39] A.A. Giunta, S.F. Wojtkiewicz, M.S. Eldred, Overview of modern design of experiments methods for computational simulations, *Proceedings of the 41st AIAA aerospace sciences meeting and exhibit*, AIAA-2003-0649. 2003.
- [40] J. Franke, A. Hellsten, H. Schlünzen, et al., *Best Practice Guideline for the CFD Simulation of Flows in the Urban Environment*, COST Action, Hamburg, 2007.
- [41] Y. Tominaga, A. Mochida, R. Yoshie, H. Kataoka, T. Nozu, M. Yoshikawa, T. Shirasawa, AIJ guidelines for practical applications of CFD to pedestrian wind environment around buildings, *J. Wind Eng. Ind. Aerod.* 96 (2008) 1749-1761.
- [42] G.E.P. Box, W.G. Hunter, J.S. Hunter, *Statistics for experimenters: an introduction to design, data analysis, and model building*[M]. New York: Wiley, 1978.
- [43] M.N. Rhode, R. DeLoach, *Hypersonic wind tunnel calibration using the modern design of experiments*, (2005).
- [44] D. Whitley, A genetic algorithm tutorial, *Stat. Comput.* 4 (1994) 65-85.
- [45] Q. Xia, X. Liu, J. Niu, K.C.S. Kwok, Effects of building lift-up design on the wind environment for pedestrians, *Indoor Built Environ.* 26 (2015) 1214 - 1231.
- [46] P.R. Spalart, Detached-eddy simulation, *Annu. Rev. Fluid Mech.* 41 (2009) 181-202.

- [47] P.R. Spalart, S.R. Allmaras, A one equation turbulence model for aerodynamic flows[J]. RECHERCHE AEROSPATIALE-FRENCH EDITION-, 1994: 5-5.
- [48] Ansys Inc, ANSYS FLUENT Theory Guide, ANSYS Inc., Canonsburg, PA, 2010.
- [49] P.R. Spalart, S. Deck, M. Shur, K. Squires, M.K. Strelets, A. Travin, A new version of detached-eddy simulation, resistant to ambiguous grid densities, Theor. Comput. Fluid Dyn. 20 (2006) 181-195.
- [50] J. Paik, F. Sotiropoulos, F. Porté-Agel, Detached eddy simulation of flow around two wall-mounted cubes in tandem, Int. J. Heat Fluid Flow 30 (2009) 286-305.
- [51] Agresti A, Kateri M. Categorical data analysis[M]. International encyclopedia of statistical science. Springer Berlin Heidelberg, 2011: 206-208..
- [52] L. Davis, Handbook of genetic algorithms, (1991).
- [53] H. Chen, R. Ooka, S. Kato, Study on optimum design method for pleasant outdoor thermal environment using genetic algorithms (GA) and coupled simulation of convection, radiation and conduction, Build. and Environ. 43 (2008) 18-30.
- [54] R. Ooka, H. Chen, S. Kato, Study on optimum arrangement of trees for design of pleasant outdoor environment using multi-objective genetic algorithm and coupled simulation of convection, radiation and conduction, J. Wind Eng. Ind. Aerod. 96 (2008) 1733-1748.
- [55] M. F. Islam, L. M. Lye. Combined use of dimensional analysis and modern experimental design methodologies in hydrodynamics experiments, Ocean Eng. 36 (2009) 237-247.
- [56] C. W. Tsang, K. C. S. Kwok, P. A. Hitchcock. Wind tunnel study of pedestrian level wind environment around tall buildings: Effects of building dimensions, separation and podium, Build. and Environ. 49 (2012) 167-181.
- [57] E. Willemssen, J.A. Wisse, Design for wind comfort in The Netherlands: procedures, criteria and open research issues, J. Wind Eng. Ind. Aerod. 95 (2007) 1541-1550.